2009

Corn stover densification using an auger compactor

Robert D. Franz
Iowa State University

Corn stover densification using an auger compactor

By

Robert D. Franz

A thesis submitted to the graduate faculty

In partial fulfillment of the requirements for the degree of

MASTER OF SCIENCE

Major: Agricultural Engineering (Advanced Machinery Engineering)

Program of Study Committee:
Stuart J. Birrell, Major Professor
Brian L. Steward
Steven J. Hoff

Iowa State University

Ames, Iowa

2009

Table of Contents

List of Figures

List of Tables

Introduction

With just over 13 billion bushels of corn produced on 86 million acres in the United States in 2007 (USDA, 2008), corn stover is the largest source of biomass in the United States. Corn stover has been collected for many years for use as feedstock and bedding in the livestock industry. It also has been used in industrial applications such as production of plastics from corn cobs. In recent years, significant research has been conducted on the harvesting of biomass for energy production. As the uses for corn stover shift from individual farm use to commercial energy production, many problems arise. There are three main focus areas in energy production from biomass: harvesting, logistics (transportation and storage), and refining. This thesis will focus on the densification of biomass to enable transportation from the field to the refinery. Due to corn stover's low bulk density, transportation costs can get very high when moving any appreciable tonnage of the material. Transportation costs have an inverse relationship with the mass of material hauled per load up to the maximum gross vehicle weight. Turhollow and Sokhansanj (2007) reported that increasing the density of the stover from 48 kg/m^3 to 74 kg/m^3, or by 54.1%, reduced transportation costs by 36.2%. Optimizing the transportation density ensures a full load while not expending extra energy to densify the material more than is necessary.

Research on corn stover densification has been focused on high density processes in recent years. Pelletizing can yield high densities at the cost of high specific energy requirements (Kaliyan and Morey, 2007). As the densities achieved by pelletization are unnecessary, so too is the extra energy associated with achieving those densities.

This thesis will explore the densification of corn stover using a compaction system requiring much less energy and yielding densities within the range of the optimal shipping

density. A low energy compaction system is a necessary component for large scale biomass refining. Balancing the transportation and densification costs is a crucial step towards the success of the biomass industry.

Literature Review

Densification is very important to the economical transport of biomass. As the density of a biomass increases, the relative cost per unit mass of biomass decreases. A density can be calculated for any given transportation system that optimizes transportation costs by maximizing the payload of the trip while not inputting more energy into densification than is necessary. The optimum transportation density can be calculated by taking the net load capacity of a vehicle and dividing it by the volume of cargo hold of the vehicle. Average vehicle dimensions yield an optimum transportation density of 234.6 kg/m^3. Various methods have been tested in regard to corn stover densification including stacking, baling, briquetting, and pelletizing.

Stackers have been used for many years to collect and package forage crops such as hay and straw as well as other feed stocks such as corn stover. Testing completed by Tuetken (2002) using a Hesston 10 Stackhand (Hesston, KS) yielded densities averaging 147.4 kg/m^3. While this was an increase to the chopped corn stover density, greater densities are still needed to make transportation affordable.

Baling has been used for many years to package forage crops into self contained units. Corn stover has been baled for many years. Baling is an effective method of densifying stover yielding densities of 128 to 160 kg/m^3 with a specific energy requirement of 2.88 to 5.76 kJ/kg (Kaminski, 1989). While baling is a tried and true technology that is well understood, it has its downfalls. Baling requires multiple passes through the field for secondary operations such as chopping, raking, baling, and collection of the bales. The multiple passes across the field from mowing, raking, and baling can cause problems with

soil compaction. Another problem with baling is contamination of the collected biomass with soil (Atchison and Hettenhaus, 2003).

Briquetting as a densification process can be achieved through a number of different methods. Briquetting dates back to 1865 when a piston briquetting machine was used to make fuel briquettes from peat (Eriksson and Prior, 1990). There are two basic steps to briquetting: compaction and agglomeration. Compaction is the application of mechanical force to reduce the volume of the material. Agglomeration is the process of creating physical bonds to hold the particles together once the compaction pressure is removed. Agglomeration can be achieved in three ways: through mechanical bonds, through the addition of supplemental binders, and through heating the material to activate its natural binders. Mechanical bonds between particles can be created when the particles are subjected to extreme pressures (.689 to 1.38 MPa) thus bringing the particles very close together and establishing bonds through the interlocking of particles or from molecular, electrostatic, and magnetic forces (Kaliyan and Morey, 2008). Alternatively, supplemental binders, such as epoxies, can be added to the material to act like glue between particles. The natural binders in the material can be activated by heating the material resulting in solid bridges between particles. Solid bridges can be formed through the partial melting of natural binders, the crystallization of soluble substances, and chemical reactions (Rumph, 1962). The binders in the material start to soften around 100°C and flow at higher temps (Eriksson and Prior, 1990). The heat needed to activate the natural binders found in corn stover can be created by subjecting the material to great pressures and thus creating heat through friction, or by adding supplemental heat to the system. There are three main types of briquetting machines: roller mill, piston, and screw briquetting machines.

A roller mill briquetting machine, shown in figure 1(a) uses a screw to compress and feed material to two counter rotating dies. The dies (figure 1(b)) are pressed together creating a large pressure that forms the briquettes. Adequate pressure is not present in a roller mill to activate the material's natural binders so additional heat must be added to the process to keep the briquettes together. To achieve proper binding the feedstock must be heated to at least 75 °C. Roller mill briquetting of corn stover can produce bulk densities as high as 463.4 kg/m^3 with a specific energy requirement of 415.5 kJ/kg (Kaliyan and Morey, 2007).

Piston-briquetting machines use a piston to compact material and push it through a die. The extreme pressures and friction created release enough heat to melt the lignin and other natural binders in the material providing agglomeration. Screw briquetting machines use a screw with either variable pitch flighting or a conical shape to continually squeeze the material together as it flows through the machine. The intense heat, between 75 and 100 °C, provided by the friction between particles and the applied pressure helps to activate natural binders in the material thus allowing the briquettes to stick together more effectively. There

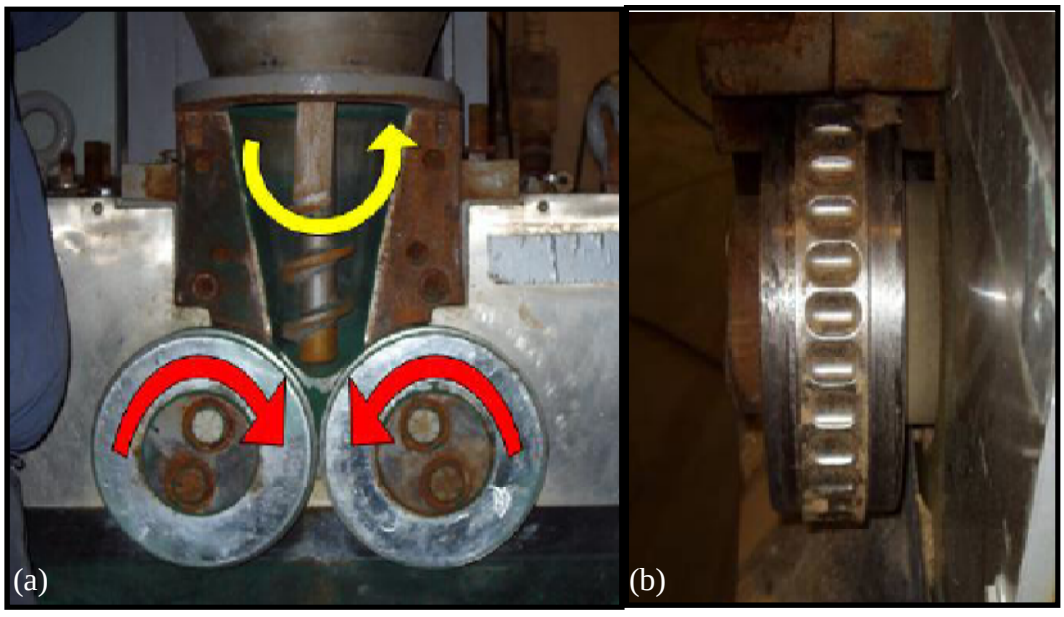

Figure 1. Cut away of a roller-mill briquetting machine and die.

has been very little research done on the densifying of corn stover using either piston or screw briquetting machines. Both machines are generally used to produce relatively large packages that are more difficult to handle than roller mill briquettes, which can be handled like grain.

Pelletizing is a similar to briquetting in that material is subjected to high pressures forming self contained units with a significantly higher density than the loose material. A pellet mill (figure 2) consists of two main sections, the steam conditioner and the die. The steam conditioner mixes steam into the biomass thereby raising the material's temperature and moisture content. The rise in temperature and moisture helps to soften the natural binders in the biomass and dissolve the soluble binders to facilitate agglomeration upon cooling and curing of the pellets. After the conditioner, the material falls to a distributing auger which feeds the material to the die. Rollers then force the material through a large number of holes bored in the perimeter of the die as shown in figure 3 (Eriksson and Prior, 1990). The temperatures needed for effective pelletization are between 75 and 100 °C with local particle temperatures often approaching 200 °C (Sokhansanj and Turhollow, 2005). The main difference between pelletizing and screw briquetting is the size of the final package: pellets are generally referred to as anything less than 30 mm in diameter (Eriksson and Prior, 1990).

The specific energy required to create pellets out of corn stover is between 189.1 and 262.3 kJ/kg depending on the moisture content and particle size. Densities of between 552.5 and 603.6 kg/m^3 can be achieved through corn stover pelletization (Kaliyan and Morey, 2007).

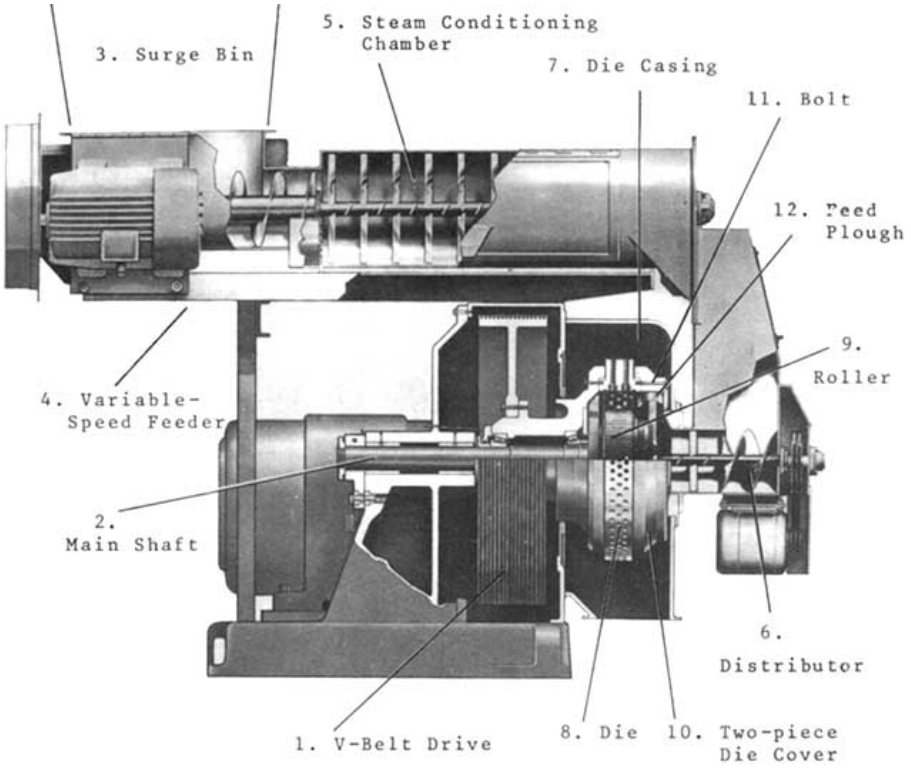

Figure 2. Cut away diagram of a pellet mill.

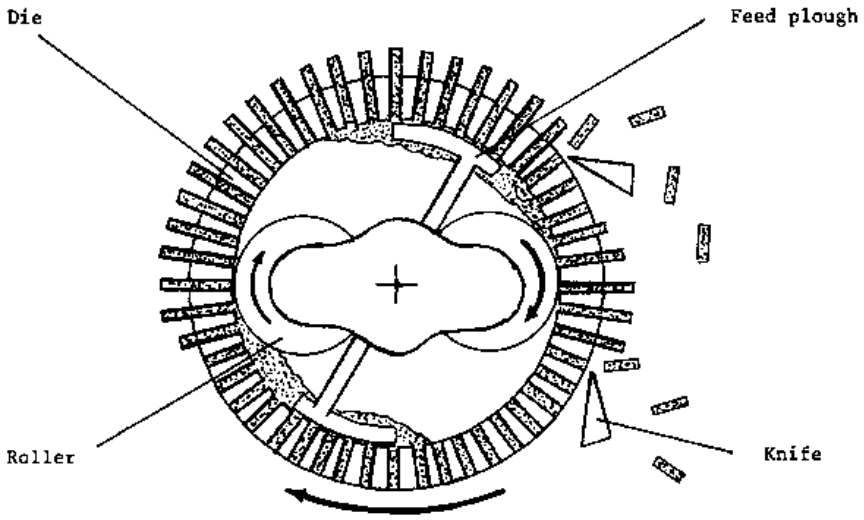

Figure 3. Cut-away diagram of a pellet mill extrusion die assembly.

All briquetting and pelletizing processes require a small particle size to operate correctly. The processes rely on heat from friction to melt the natural binders in the biomass and hold the finished briquette together. The heat is generated by particles of material moving past each other. Thus, the flowability of the material is very important. An effective way to increase the flowability of the material is to decrease its particle size. To reduce the particle size of the harvested stover to meet these requirements, the material must be subjected to a milling process. Milling operations invariably require a large amount of energy and therefore add a significant cost to the densifying of the material. Research by Dilts (2007) yielded milling specific energies of between 45.46 KJ/kg and 106.98 KJ/kg depending on the size of screen and feed-rate used with corn stover in a hammermill. Mani et al. (2004) found specific energies of between 25.2 kJ/kg and 79.2 kJ/kg for particle size reduction of corn stover using a hammermill.

Table 1. Summary of densities and specific energies for selected densification processes.

Method	Density, kg/m^3	Specific Energy, kJ/kg
Stacking	147.4	N/A
Baling	160	5.76
Briquetting	463.4	415.5
Pelletizing	603.6	262.3

While conventional briquetting and pelletizing are poor options when dealing with large particulate matter, the same principles of extrusion may be applied. An auger system could be used not only to convey the material but also to compact it. Screw conveyors have been used to transport a wide array of materials from liquids to particulate matter to fibrous material. The energy associated with conveying material was studied by Degirmencioglu and Srivastava (1996). Through dimensional analysis, Degirmencioglu and Srivastava were able to construct a specific power model for conveying grains as shown in equation 1.

$$\frac{P/L}{Q\rho g} = 23.03\left(2\pi n\sqrt{\frac{l_p}{g}}\right)^{0.178}\left(\frac{d_{sf}}{l_p}\right)^{-9.115}\left(\frac{c}{d_p}\right)^{-0.344}\left(\frac{l_i}{l_p}\right)^{0.162}$$

$$\times (1.46 - cos^2(\theta))^{1.051}(\mu_2)^{1.84} \qquad \textbf{(Eqn. 1)}$$

Where: P = Power, W; L = Length of flighting, m

Q = Volumetric capacity (m^3/s); ρ = Material bulk density (kg/m^3)

g = Acceleration of gravity (m/s^2); n = Screw speed (rev/s)

l_p = Pitch (m); d_{sf} = Screw flighting diameter (m)

c = Screw clearance (m); d_p = particle diameter (mm)

θ = Screw angle of inclination (deg); l_i = Exposed screw intake length (m)

μ_2 = Material/material coeff. of friction (dimensionless)

Conveying wheat yielded specific energies per unit length conveyed of 19.62 J/kg-m using the Degirmencioglu model. Zhong and O'Callaghan (1990) found a specific energy of 32.35 kJ/kg when using a screw conveyor to move chopped hay. Merritt and Mair (2008) derived a model of the torque in a screw conveyor based off of the shear stress imparted on the inside surface of the screw casing by the flowing material as shown in equation 2.

$$T = \frac{\pi}{2} L_F {D_C}^2 \tau_C \cos\phi \qquad \textbf{(Eqn. 2)}$$

Where: T = Torque (N-M); L_F = Length of the flighting (m)

D_C = Diameter of the casing (m); τ_C = Casing shear stress (N/m^2)

ϕ = Flow angle of the material relative to the inner casing surface (deg)

The torque from the Merritt model can yield a specific energy using the speed of the shaft and the mass flowrate of the material.

Using an auger to provide the compaction force necessary to densify the stover could create a very simple machine capable of producing high bulk density stover for economical transport. Auger compaction of large particle corn stover requires more research. A low cost method of densifying stover will be an important component in the future success of the biomass industry. The need for a densification method that does not require a large energy input is needed to further advance the biomass harvesting and refining industry.

Objectives

The main goal of this study was to design and test an auger compactor capable of densifying corn stover without particle size reduction beyond what a harvester can provide. Two auger designs were explored; a constant pitch system and a variable pitch system. More specifically the objectives were as follows:

- Design and build an auger compaction test stand,
- Determine a model relating the density and compaction pressure in an auger compaction system. Evaluate different forms of the model to find which is the most accurate,
- Determine a model relating the specific energy of compaction to the compaction pressure in an auger compaction system. Compare the results to other technologies to determine feasibility of the system, and
- Investigate the feasibility of a variable pitch auger compacter in densifying corn stover.

Apparatus, Methods & Procedures

The development of the auger compaction system, the data acquisition system, the materials, and the procedure will be discussed below.

Development of auger compaction system

The biomass compacter was designed and built in the Agricultural and Biosystems Engineering Department at Iowa State University. The compactor consisted of two halves, the auger unit and the collection tube. Material was fed in to the machine via the hopper located on the auger unit as shown in figure 4. The material then fell into the flighting of a 0.3048 m diameter auger with a .1143 m center shaft, a 0.3048 m pitch and 9.53 mm thick flighting (figure 5). The auger was powered by a Char Lynn 6000 Series 491.6 cm^3/rev geroler disk valve hydraulic motor (Eaton Corporation, Cleveland, OH) via an in-line planetary gear set with a gear ratio of 2.7143. The material was conveyed 2.134 m along the length of the auger until it reached the collection tube.

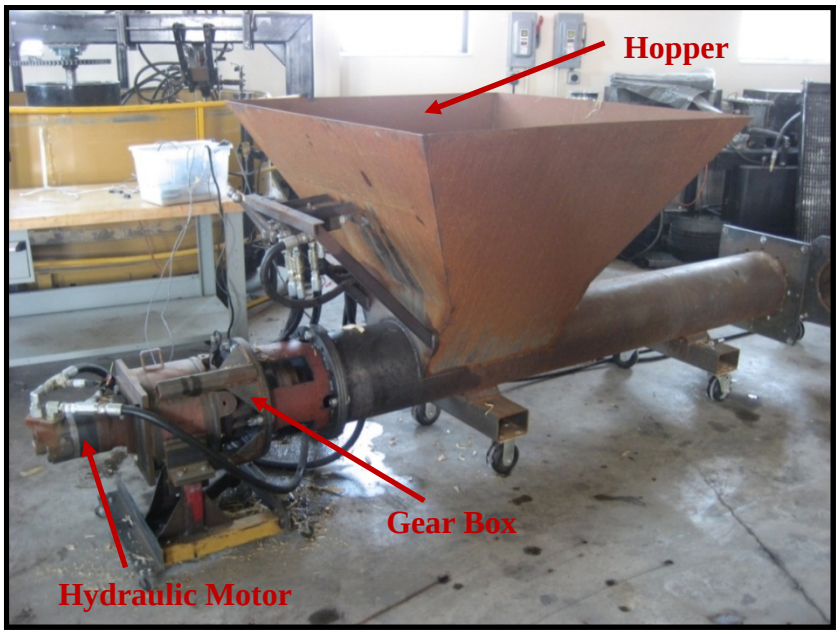

Figure 4. Image of the auger unit of the auger compaction system.

Figure 5. View of the auger from inside the hopper of the auger compaction system.

The collection tube (figure 6) contained a ram that was attached to a hydraulic cylinder that provided both a resistive force to the ram during operation and also a means of ejecting the sample after a test. The resistive force on the ram was controlled using the hydraulic circuit shown in figure 7. The directional control valve was shifted down to provide pressure to the rod end of the cylinder. The pressure at the cap end of the cylinder was held constant by a variable pressure relief valve. The force on the ram was varied by adjusting the proportional pressure relief valve and thus adjusting the pressure difference between the ends of the cylinder. The adjustment in the proportional pressure relief valve allowed for extension, retraction, or equilibrium in the cylinder. The proportional relief valve was controlled by a pulse width modulation (PWM) signal produced by a digital PWM generator (Critical Velocity Enterprises, LLC,New York, NY) through the data acquisition system interface.

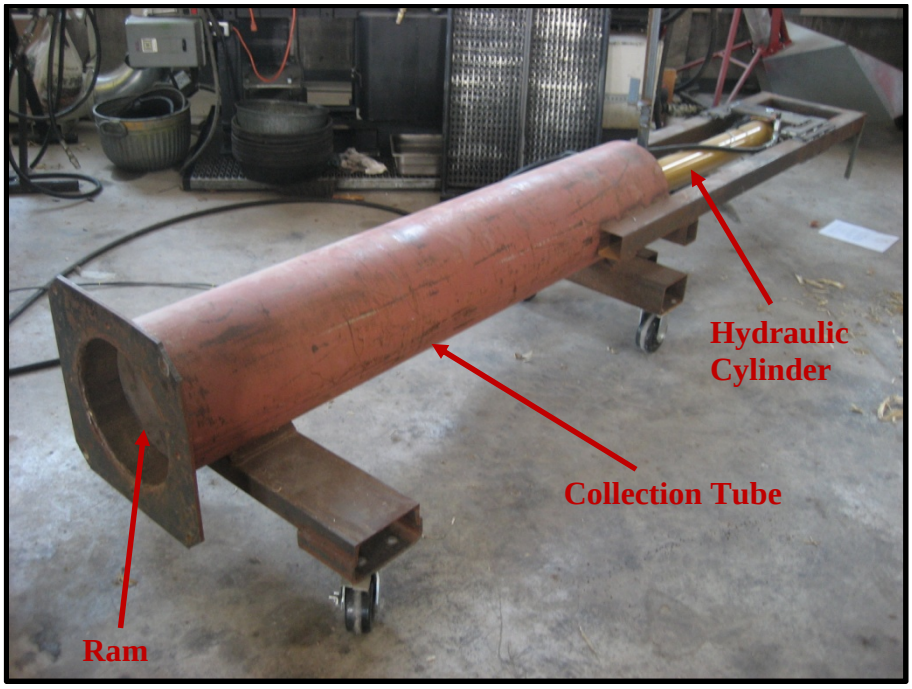

Figure 6. Image of the collection tube of the auger compaction system.

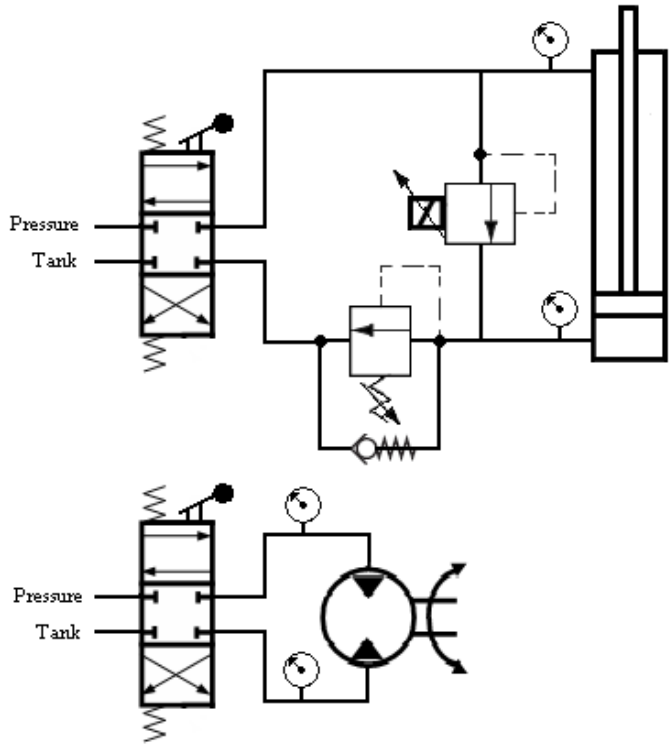

Figure 7. Schematic of the hydraulic system on the auger compaction system.

Data Acquisition

The data acquisition system included a Microsoft Windows based laptop, two USB data acquisition units (USB1208-LS Personal Measurement Device, Measurement Computing Corporation, Norton, MA), a power supply, four pressure transducers, a magnetic pickup sensor, and a laser distance sensor. The PMDs' features include digital I/O circuits, analog I/O circuits, and an event counter. The PMDs served as an interface between the laptop and the various sensors and controls. Data was collected from the system and stored on the laptop using an interface developed with Microsoft Visual Basic. The Visual Basic interface provided the user with control of the compaction pressure and method of consistently recording data for future analysis.

Pressure transducers (PX 319-5KG5V, Omega Engineering, Inc., Stamford, Connecticut) were used to measure the pressure drop across the motor and the cylinder in the system. Pressure transducers were placed at both the high and low ports of the motor and at both the rod and cap ends of the cylinder. All of the pressure transducers were rated for 0 to 34.473 MPa (5000 psi). The measurements gained from these sensors along with a published efficiency for the motor helped to provide an accurate measure of torque in the motor and thus the torque in the auger shaft. The force in the cylinder was also calculated from the data gained from the pressure transducers along with experimentally derived internal cylinder frictions.

The auger shaft speed was sensed using a magnetic pickup sensor (Cherry MP1005, ZF Electronics Corporation, Auerbach, Germany). The magnetic pickup sensor was placed above a 40-tooth sprocket mounted on the auger shaft as shown in figure 8. The shaft speed was calculated using the frequency of the pulses generated by the magnetic pickup sensor

Figure 8. Shaft mounted sprocket and magnetic auger speed pickup sensor for the compaction system.

every time one of the sprocket's teeth passed. The shaft power was calculated using the shaft speed and torque.

An accurate measurement of the displacement of the ram was needed to measure the density of the final sample. A laser distance sensor (Efector O1D100, IFM Efector, Exton, PA) was mounted behind the ram and measured the distance to the ram, providing real-time ram displacement. A tape measure was used to measure the ejected length of each sample. Each sample was weighed using a scale (Easy Weigh BX-300+, Atron Systems Inc., West Caldwell, NJ).

Material

The biomass used in the tests originated in the form of large square cornstalk bales harvested in the fall of 2008 and stored under cover. After harvest, the residue in a corn field was chopped with a flail chopper, raked, and baled into 3 x 3 x 6 large square bales. In

a practical application the stover would be harvested using a single pass biomass harvester with a double shear chopper. To simulate the properties of material that had been harvested with a combine containing a double shear chopper, the bales were broken and fed through a John Deere 9750 STS combine with a double shear chopper and a blower mechanism**.** After exiting the combine the material was collected in a forage wagon.

Design of Experiment

A randomized block design was used where each of six treatments were randomly tested in a "block." Five blocks were completed resulting in five repetitions for each treatment. The reasoning for a randomized block design was to isolate the effects of varying the compaction pressure by eliminating the effects of variables in the process that cannot be controlled and may change over time such as moisture and other changes in the material. Six treatments were used and consisted of different compaction pressure settings of 0, 6.89, 13.79, 27.58, 55.16, and 110.32 kPa (0, 1, 2, 4, 8, and 16 psi).

Procedure

An exact procedure was followed for every test within the experimental design. The details of this procedure will be discussed below.

The first step in the procedure was to measure out 18.14 kg of stover using the large scale. The stover was measured 2.27 to 3.18 kg at a time and loaded into the hopper. Since the ram tended to rotate during tests, it was returned to a standard alignment before each test to enhance consistency. The ram alignment is shown in figure 9.

Figure 9. Alignment of the ram using the arrows on the right side.

Once the ram was properly aligned, it was moved back into the collection tube and the two halves of the machine were bolted back together. The ram was then moved all the way forward. The ram pressure was set through the computer interface to within ±0.69 kPa (0.1 psi) of the desired nominal ram pressure setting. Data logging was started and the motor engaged. Stover was fed until the displacement of the ram reached .381 meters as measured by the laser distance sensor from the back of the ram or until the motor stalled. Once the final displacement was reached the auger was disengaged, the data acquisition was stopped, and the compaction pressure cylinder shifted into neutral. The sections were then unbolted, the collection tube clamped to the ejection trough, and the sample ejected. As the sample was ejected, a piece of plywood was held to the end of the sample to keep it together so as to yield an accurate post ejection length (figure 10(a)). Using the ram and the piece of plywood as end points the expanded length of the sample was measured using a tape measure (figure 10(b)).

Figure 10. Using a piece of plywood to ensure an accurate ejected length

The ejected sample's weight was then measured and recorded. Any material lost during the separation of the halves and ejection was collected and weighed. The material from the first flight of the auger was also collected and weighed. Adding the volume and mass of the material from the first flight of the auger provided a constant method for calculating density. Once all of the measurements were taken, the hopper was cleaned out and the auger unit emptied of material to provide a constant starting point for all tests.

Theoretical Model

A theoretical model for the system was developed based on the literature review and physics principles. The literature review yielded three models for the density vs. compaction pressure relationship. A model for the specific energy vs. compaction pressure was derived using research from the literature review and a force analysis of system components. These models will be described below.

Density vs Compaction Pressure

Various studies have been conducted over the years establishing a relationship between density and pressure in corn stover and other biomaterials. The first and most prevalent model shows a logarithmic relationship between the density and pressure as shown in eqn. 3 below (Mani, et al., 2003). There have been many iterations of this equation over the years; however it remains a logarithmic relationship.

$$\gamma = m \log P + c \qquad \textbf{(Eqn. 3)}$$

Where:

γ = material bulk density, kg/m^3 P = compaction pressure, kPa

c = constant, kg/m^3 m = material compressibility

Research by Kaminski (1989) concerning densification of biomass yielded a power relationship as shown in eqn. 4.

$$\gamma = k(P)^n \qquad \textbf{(Eqn. 4)}$$

Where: k = constant n = constant

The k term is related to the length of the cut and the amount of cobs in the material. The n term is related to the length of the cut and the moisture content of the material. Kaminski also noted other factors that affect the unloaded bulk density of the material such as dwell time,

moisture content, and speed of the applied load. Frohberg (2005) added a known initial bulk density term, γ_0, to the Kaminski equation to yield the eqn. 5 as shown below.

$$\gamma = k \times P^n + \gamma_0 \qquad \textbf{(Eqn. 5)}$$

The addition of the known initial density term provided a more accurate model of the relationship between density and pressure extending all the way to zero pressure, something log-based models cannot achieve.

Specific Energy vs Compaction Pressure

The specific energy model for the system can be broken up into three parts: the specific energy due to feeding and conveying the material from the hopper to the compaction tube, the specific energy due to compaction of the material, and the specific energy needed to overcome friction forces in the collection tube as shown in figure 11.

The feeding and conveying portion of the equation (E_{FC}) can be broken up into two parts, the cutting or feeding energy (E_F) and the conveying energy (E_{Cvy}). The cutting force represents the amount of energy it takes to shear off the material as it moves from the hopper to the tube of the auger unit and will by ignored in our analysis. The conveying component

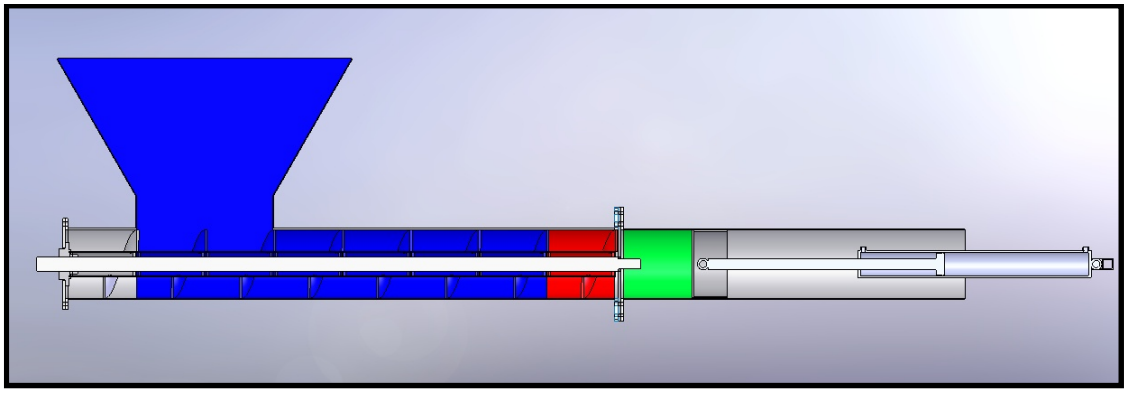

Figure 11. A cutaway of the compactor showing the three sections for the energy model. Blue - Feeding and conveying; Red – Compacting; Green – Friction

represents the amount of energy it takes to move material from the hopper to the collection tube on a per kilogram basis. To calculate the specific energy it is necessary to first find the torque. Equation 6 gives the conveying torque as given by Merritt and Mair (2008).

$$T_{Cvy} = \frac{\pi}{2} L_F {D_C}^2 \tau_C \cos\phi \qquad \textbf{(Eqn. 6)}$$

Where: L_F = Length of flighting, m D_C = Diameter of screw casing, m

τ_C = Casing shear stress, Pa ϕ = Material flow angle, deg

The material flow angle is described as the direction of the flow of material relative to the casing surface (Merritt and Mair, 2007). The casing shear stress and the flow angle are both properties of the material that are very difficult to estimate and vary depending on conditions within the auger casing. Due to difficulties in measuring the casing shear stress and the flow angle of the material, they will be considered as one parameter, $\tau_C \cos\phi$, in this analysis. The energy used in conveying the material can be found by multiplying the torque by 2π times the number of revolutions as shown in eqn. 7.

$$E_{Cvy} = T_{Cvy} \cdot 2\pi \cdot rev \qquad \textbf{(Eqn. 7)}$$

Where: rev = Number of revolutions

Substituting for T_{Cvy} from eqn. 6 into eqn. 7 yields the conveying energy (eqn. 8).

$$E_{Cvy} = \left(\frac{\pi}{2} L_F {D_C}^2 \tau_C \cos\phi\right) 2\pi \cdot rev \qquad \textbf{(Eqn. 8)}$$

The next major component of the system is the energy it takes to compact the material. This energy is based off of the amount of torque the auger experiences due to the compaction pressure on the material along with the mass of the material compacted. The first step to modeling the compaction energy is to find an equation giving the torque. The torque needed to compact that material depends on four different factors: the angle of the

flighting (θ), the radius of the flighting (r), the coefficient of friction between the flighting and the material (μ_F), and the force on the face of the flighting from the ram (F_y). When calculating the amount of torque that an auger experiences it is important to realize that the flighting on the auger can be looked at as an inclined plane with a slope θ. The slope of a helical surface depends on the pitch of the flighting, H, and continuously varies at any radius from the axis of the helix as described in eqn. 9

$$\theta = \tan^{-1}\left(\frac{\pi r}{2H}\right) dr \qquad \textbf{(Eqn. 9)}$$

From figure 12 the following force equations can be derived.

$$F_x = F_N \cos\theta - F_f \sin\theta \qquad \textbf{(Eqn. 10)}$$

$$F_y = F_N \sin\theta - F_f \cos\theta \qquad \textbf{(Eqn. 11)}$$

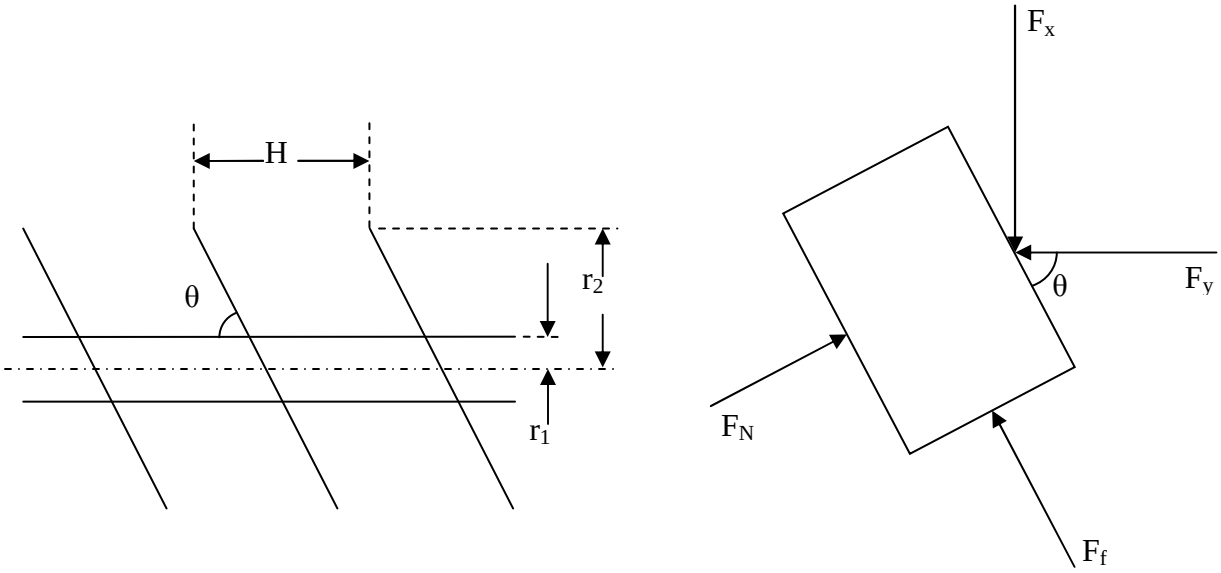

Figure 12. Diagram of the auger and a free-body diagram of a unit of stover.

The friction force F_f is a function of the normal force F_n as show in eqn. 12

$$F_f = \mu_F F_N \qquad \textbf{(Eqn. 12)}$$

Thus eqn. 11 can be rewritten as shown below.

$$F_N = \frac{F_y}{\sin\theta - \mu\cos\theta} \quad \textbf{(Eqn. 13)}$$

Substituting eqns. 12 and 13 into eqn. 10 yields eqn. 14.

$$F_x = F_y\left(\frac{\cos\theta - \mu_F \sin\theta}{\sin\theta - \mu_F\cos\theta}\right) \quad \textbf{(Eqn. 14)}$$

By using eqn. 9, and some basic trigonometric identities, eqns. 15 and 16 can be derived.

$$\cos\theta = \left(\frac{2H}{hyp.}\right) \quad \textbf{(Eqn. 15)}$$

$$\sin\theta = \left(\frac{\pi r}{hyp.}\right)dr \quad \textbf{(Eqn. 16)}$$

Substituting eqns. 15 and 16 into eqn 14 yields eqn. 17.

$$F_x = F_y\left(\frac{2H - \mu_F\pi r}{\pi r - \mu_F 2H}\right)dr \quad \textbf{(Eqn. 17)}$$

Torque, T, can be written as the product of the force in the x direction and the radius.

$$dT = F_x \cdot r \quad \textbf{(Eqn. 18)}$$

By substituting in for F_x the torque is given as a function of the force from the ram, F_y.

$$dT = F_y\left(\frac{2H - \mu_F\pi r}{\pi r - \mu_F 2H}\right)dr \cdot r \quad \textbf{(Eqn. 19)}$$

Integrating the torque over the width of the flighting as shown in eqn. 20 yields torque as a function of the force in the y direction, eqn. 21.

$$T = F_y\int_{r_1}^{r_2} r\left(\frac{2H - \mu_F\pi r}{\pi r - \mu_F 2H}\right)dr \quad \textbf{(Eqn. 20)}$$

$$T = F_y\frac{A+B+C}{2\pi^2} \quad \textbf{(Eqn. 21)}$$

Where:

$$A = 8H^2\mu_F({\mu_F}^2 - 1)\ln\left|\frac{2H\mu_F - r_1\pi}{2H\mu_F - r_2\pi}\right| \quad \textbf{(Eqn. 22)}$$

$$B = \pi 4H(r_1 - r_2)({\mu_F}^2 - 1) \quad \textbf{(Eqn. 23)}$$

$$C = \pi^2\mu_F({r_1}^2 - {r_2}^2) \quad \textbf{(Eqn. 24)}$$

To estimate the torque as a function of compacting pressure from the ram it is necessary to find the axial force of the ram onto the material and then distribute that force across the area of the flighting. This can be done by multiplying the compaction pressure by the ratio of the areas of the ram and the first flight of the auger, R_A as shown in eqn. 25.

$$R_A = \frac{a_{ram}}{a_{flighting}} = \frac{\pi \cdot {r_{ram}}^2}{\pi({r_2}^2 - {r_1}^2)} \quad \textbf{(Eqn. 25)}$$

As with the conveying energy, the torque must be multiplied by 2π times the number of revolutions, yielding the total energy from compaction as shown in eqn. 26.

$$E_{Compact} = \left(P_{ram} \cdot R_A \frac{A+B+C}{2\pi^2}\right) \cdot 2\pi \cdot rev \quad \textbf{(Eqn. 26)}$$

Where: P_{ram} = Compaction pressure on the face of the ram, kPa

The last part of the model deals with the friction of the compacted sample in the collection tube. This friction specific energy is based on the pressure that the material exerts on the tube, P_T, the coefficient of friction between the material and the tube, μ_T, and the displacement of the ram, L_d. As with the other energies the friction energy must first be expressed as a torque as shown in eqn. 27.

$$T_{Friction} = \frac{\pi}{2} L_d {D_C}^2 \mu_T P_T \quad \textbf{(Eqn. 27)}$$

Where: L_d = Ram displacement, m D_c = Diameter of the collection tube, m

μ_T = Material/tube coeff. of friction P_t = Pressure on inside of tube, Pa

The torque must be multiplied by 2π times the associated number of revolutions yielding the total energy from friction as shown in eqn. 28.

$$E_{Friction} = \left(\frac{\pi}{2} L_d {D_C}^2 \mu_T P_T\right) \cdot 2\pi \cdot rev \quad \textbf{(Eqn. 28)}$$

By combining eqns. 8, 26, and 28 we get the total energy as shown in eqn. 29.

$$E_{Total} = \left(\frac{\pi}{2} L_F {D_C}^2 \tau_C \cos\phi\right) 2\pi \cdot rev$$

$$+ \left(P_{ram} \cdot \mathrm{R_A} \frac{8H^2 \mu_F (\mu_F{}^2 - 1) \ln\left|\frac{2H\mu_F - r_1\pi}{2H\mu_F - r_2\pi}\right| + \pi 4H(r_1 - r_2)(\mu_F{}^2 - 1) + \pi^2 \mu_F (r_1{}^2 - r_2{}^2)}{2\pi^2} \right) \cdot 2\pi \cdot rev$$

$$+ \left(\frac{\pi}{2} L_d {D_C}^2 \mu_T P_T\right) \cdot 2\pi \cdot rev \qquad \textbf{(Eqn. 29)}$$

The specific energy can be calculated by dividing the total energy by the total mass of material compacted as shown in eqn. 30.

$$SE = \frac{E_{Total}}{M} \qquad \textbf{(Eqn. 30)}$$

Where: M = Total mass of compacted material.

Data Analysis

The collected data consisted of hydraulic pressures, shaft speed, and ram displacement. To get the data into a meaningful state it was manipulated to yield more useful quantities such as torque and energy.

To assure accuracy, the pressure transducers were calibrated prior to data analysis. The first step in calibrating the sensors was to plumb them together with a new 0-2,758 kPa needle gauge as shown in figure 13.

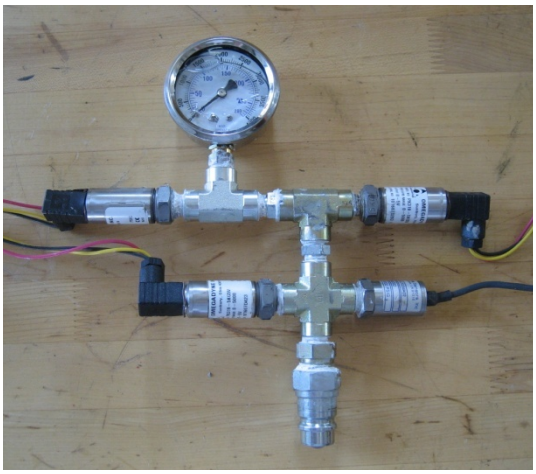

Figure 13. Pressure sensor cluster for calibration of Pressure Transducers

Plumbing the sensors together ensured that all of the sensors experienced the same pressure. The pressures were varied from 1724 kPa to 8274 kPa in 689 kPa intervals. Once the pressure was set, readings were taken at steady state for one minute before adjusting to a new pressure. Average pressures were found for each sensor over a period of 40 seconds of steady state operation for each pressure setting. The average pressures were plotted against the real pressures and linear trend lines fit to the data for each sensor resulting in calibration curves.

Since the main focus of this thesis was to establish relationships between different system characteristics and the compaction pressure from the ram, it was necessary to find average values for the compaction pressure for each run. These pressures were used in comparisons with both the density and the specific energy. The cap and rod end pressures from the cylinder along with the internal cylinder friction were used to calculate the force in the cylinder as shown in equation 31. The internal cylinder friction was found by measuring the amount of force needed to move the cylinder.

$$F_{Cyl} = \left(P_{Cap} \cdot A_{Cap}\right) - \left(P_{Rod} \cdot A_{Rod}\right) - F_{Cyl\ Friction} \qquad \textbf{(Eqn. 31)}$$

A positive resultant force relates to an extending force in the cylinder. Once calculated, the force was divided by the total face area of the ram to get compaction pressure as shown in eqn. 32.

$$P_{Ram} = \frac{F_{Cyl}}{\pi(r_{ram})^2} \qquad \textbf{(Eqn. 32)}$$

The parameters for the cylinder can be found in table 2. Once the instantaneous compaction pressures were calculated, an average was taken over the operating span of the test run.

Table 2: Specifications of the ram cylinder of the auger compaction system

Cylinder Bore	10.16 cm
Rod Diameter	5.08 cm
Cap-end Area	81.07 cm^2
Rod-end Area	60.80 cm^2
Ram radius	30.48 cm
Cylinder Friction	534 N

To assess the torque on the shaft of the auger unit, the torque in the motor needed to be calculated. A formula for finding the torque in a hydraulic motor is shown in equation 33.

$$T = \frac{\Delta P \cdot D_m}{2 \cdot \pi} \cdot \eta_{Motor} \quad \textbf{(Eqn. 33)}$$

where: T = Motor torque (N-m)

ΔP = Pressure drop across the motor (MPa)

D_m = Displacement of the motor (cm^3/revolution)

η_{Motor} = Torque efficiency of the motor (dimensionless)

Once the motor torque was found it was multiplied by the gear ratio of the gearbox to find the shaft torque, T_{Shaft} as shown in eqn. 34.

$$T_{Shaft} = T_{Motor} \cdot GR \cdot \eta_{Gearbox} \quad \textbf{(Eqn. 34)}$$

where: T_{Shaft} = Shaft torque (N-m)

GR = Gear ratio of the gearbox (dimensionless)

$\eta_{Gearbox}$ = Torque efficiency of the gearbox (dimensionless)

The speed of the auger shaft was calculated using the magnetic pickup sensor mounted to sense the teeth of a sprocket mounted on the auger shaft. The speed was recorded at 10 samples per second and averaged every twenty readings over the length of the run. The specifications of the auger drive train can be found in Table 3.

Table 3. Auger drive train specifications for the auger compaction system.

Motor Displacement	491.6 cm^3/revolution
Torque Efficiency – Motor	0.873 (dimensionless)
Gear ratio	2.71 (dimensionless)
Torque Efficiency – Gearbox	0.98 (dimensionless)
Number of teeth on sprocket	40 teeth

To find the specific power of a run, the first step is to find the average speed and torque through the compaction portion of the run. The average torque was multiplied by 2π times the average speed in revolutions per minute, and the duration of the run in minutes. This yielded the total compaction energy from the run. The total compaction energy was then divided by the total mass of the material to yield the specific energy. The specific energy was evaluated from the time the ram started to move, thus the start of compaction, until the auger was stopped. This procedure along with all of the data analyzing procedures were written into a Visual Basic for Applications (Microsoft Corporation, Redmond, WA) program. This allowed for consistency in the data analysis.

Once the compaction pressures and specific energies were calculated for all of the tests, the statistics package JMP (SAS, Cary, NC) was used to perform a statistical analysis on the data including an ANOVA analysis based on the six nominal pressure settings and non-linear regressions of the density versus compaction pressure and specific energy versus compaction pressure data.

Results and Discussion

Testing of the auger compacter yielded quantitative results. The results of the calibration will be discussed first followed by the results of an ANOVA statistical analysis of the data and fitting models to the data using a non-liner regression.

The calibration was performed and it was found that the cap-end pressure transducer from the cylinder was perfectly calibrated with the needle gauge. The other sensors provided calibration curves as shown in figure 14.

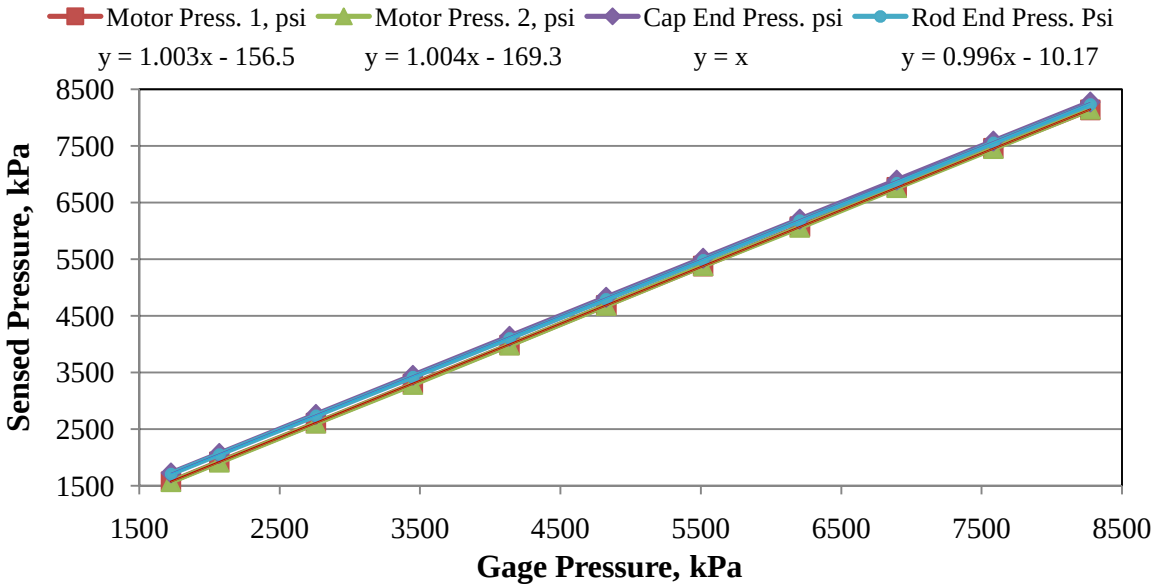

Figure 14. Pressure sensor transducer calibration curves.

An ANOVA analysis was performed using JMP on the density, the relaxed density, and the specific energy data based on the six treatments in the experimental design. The ANOVA analysis tested for significance at the 0.05 level. The results are given in table 4 below with the compaction pressure coming from the actual measured pressures from the tests.

Table 4. Means (and standrad deviations) for all treatments, including final constrained density, relaxed unconstrained density, specific energy of compaction and percent of total biomass energy utilized for compaction.

Compaction Pressure	Density[1]	Relaxed Density[1]	Density Reduction	Specific Energy[1]	Percentage of energy in the material*
kPa	kg/m3	kg/m3	%	kJ/kg	%
15.28 (±13.02)	170.92 (±7.2)[a]	130.69 (±5.75)[a]	-23.54	17.69 (±6.47)[a]	0.09
20.37 (±7.27)	171.83 (±29.55)[a]	128.6 (±24.51)[ab]	-25.16	15.43 (±2.31)[a]	0.08
24.45 (±3.22)	214.77 (±26.28)[b]	154.45 (±11.68)[bc]	-28.08	21.51 (±6.52)[ab]	0.11
38.66 (±6.1)	248.64 (±34.01)[b]	165 (±16.46)[c]	-33.64	23.61 (±6.68)[ab]	0.12
63.08 (±5.45)	297.5 (±26.31)[c]	208.11 (±15.35)[d]	-30.05	29.35 (±8.31)[bc]	0.15
116.86 (±4.61)	342.59 (±36.09)[d]	235.17 (±25.28)[e]	-31.36	35.17 (±6.3)[c]	0.18

[1]Different letters indicate a significant difference at 95% confidence. *Based on 20 MJ/kg total energy of biomass.

In all of measurements evaluated there was no significant difference between the 0 and 6.89 kPa treatments. The lack of significant difference between the lower treatments can be explained by the fact that the relative difference in the pressure setting is quite small in the smaller treatments and the variance in the system overshadows that difference in nominal pressure settings.

The specific energy data yielded no significant difference between the 0, 6.89, 13.79, and 27.58 kPa treatments. Only three significantly different groups were present in the specific energy data with overlap present in all of the groups. The small number of significant groups can be attributed to the amount of variance in the system relative to the average increase in the specific energy between treatments.

After the ANOVA analysis proved that there was a significant difference in the data between treatments, a non-linear regression was performed using JMP based off of the following logarithmic and power models as shown in eqns. 35, 36, and 37.

$$\gamma = m \log P + C \quad \textbf{(Eqn. 35)}$$

$$\gamma = K \times P^n + \gamma_0 \text{ (Frohberg)} \quad \textbf{(Eqn. 36)}$$

$$\gamma = K \times P^n \text{ (Kaminski)} \quad \textbf{(Eqn. 37)}$$

A logarithmic relationship was established between density and compaction pressure by Burmistrova (1963). However, the logarithmic relationship provides a poor representation at low pressures due to a logarithmic function's tendency to go asymptotically negative as the pressure approaches zero. Kaminski's model gives a more accurate model as the density goes to zero as the pressure approaches zero. Frohberg's model is the same as Kaminski's only it allows for a positive and realistic initial density when the pressure approaches zero.

Figure 15 shows the observed data with all three models shown.

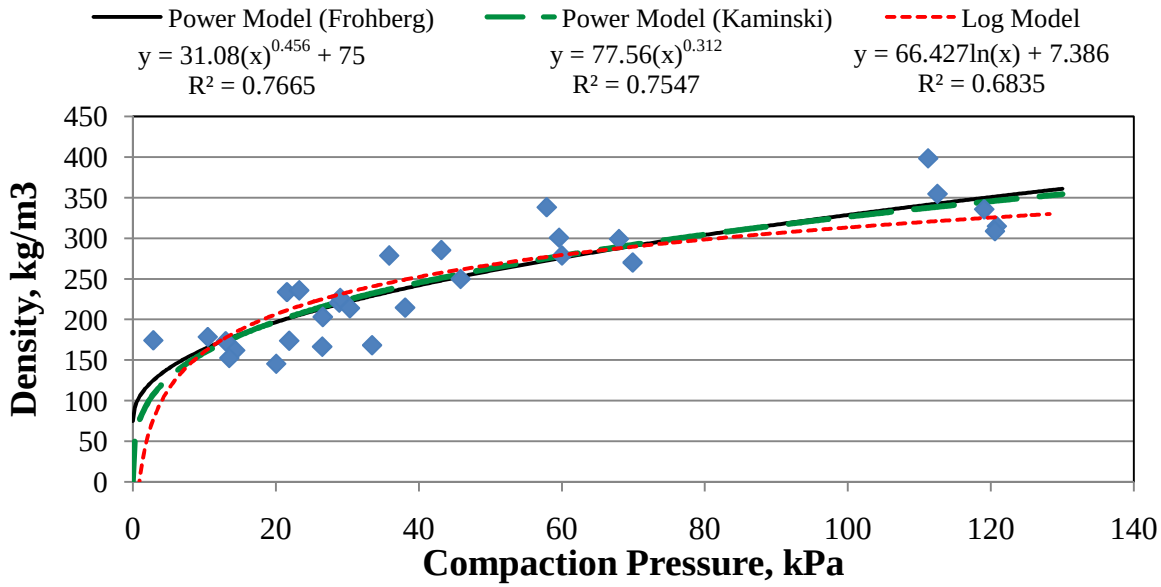

Figure 15. Plot of the final compacted density vs. compaction pressure with the logarithmic, Kaminski, and Frohberg regressions.

The Frohberg model yielded a better fit to the acquired data as indicated by the root mean square error of the model from the non-linear regression and shown in table 5. Due to the models having the same number of parameters the R^2 values can be compared. The Frohberg model has a higher R^2 than either the logarithmic model or the Kaminski model and thus is more statistically significant. The significance of the model parameters are shown in table 6.

All of the parameters have a p-value of less than .0001 indicating high levels of significance except for the C parameter in the logarithmic model. Both the Kaminski and Frohberg model's parameters are highly significant. However, due to the Frohberg model's higher R^2 value it can be shown that the Frohberg model is the best fit.

Table 5. Statistical analysis of the pressure vs. density models.

Model Significance			
Model	Regression	Model DOF	R^2
Logarithmic	Non-Linear	2	0.6835
Power (Kaminski)	Non-Linear	2	0.7547
Power (Frohberg)	Non-Linear	2	0.7665

Table 6. Parametrical significance of the density vs. pressure models.

Parametrical Significance			
Parameter	Model	Value	P-value
m	Logarithmic	66.43	<.0001
C	Logarithmic	7.39	0.2202
K	Power (Kaminski)	77.56	<.0001
n	Power (Kaminski	0.312	<.0001
K	Power (Frohberg)	31.08	<.0001
n	Power (Frohberg)	.456	<.0001

When ejected from the collection tube the material held a cylindrical shape while expanding axially. The density of the ejected samples ranged from 130.6 kg/m^3 to 235.1 kg/m^3 as shown in figure 16. Plotting the relaxed vs. compacted densities shows a close linear relationship as shown in figure 17.

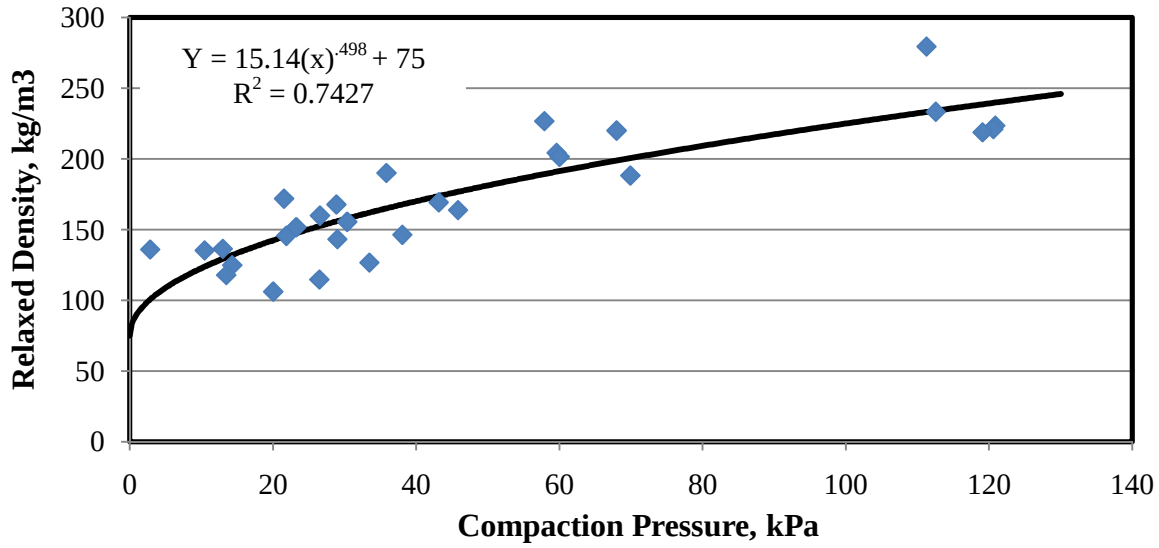

Figure 16. Plot of the relaxed density vs. the compaction pressure with the Frohberg regression line shown.

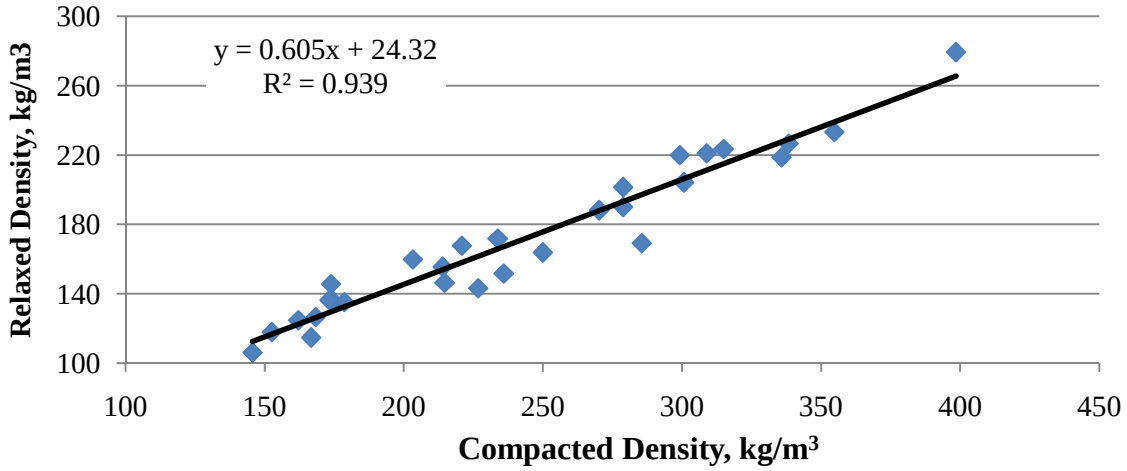

Figure 17. Plot of the relaxed vs. compacted densities with the expansion curve

The ejected sample had many characteristics mimicking those of a square bale with its strings cut. While square bales have slices, the compacted "logs" consisted essentially of a corn stover mat in the shape of a helix. In this way the log was essentially sliced. These slices held together well even after the helix was broken apart. These properties leave room for multiple avenues of handling in the future. One option is to leave the material unbound meaning that the "logs" could break apart and moved as a bulk material. Another option would be to externally bind the "logs" together creating long cylindrical bales that would be handled as individual units.

Figure 18 shows a plot of the observed compaction pressure versus specific energy. Based on the theoretical model for the specific energy a linear relationship can be established.

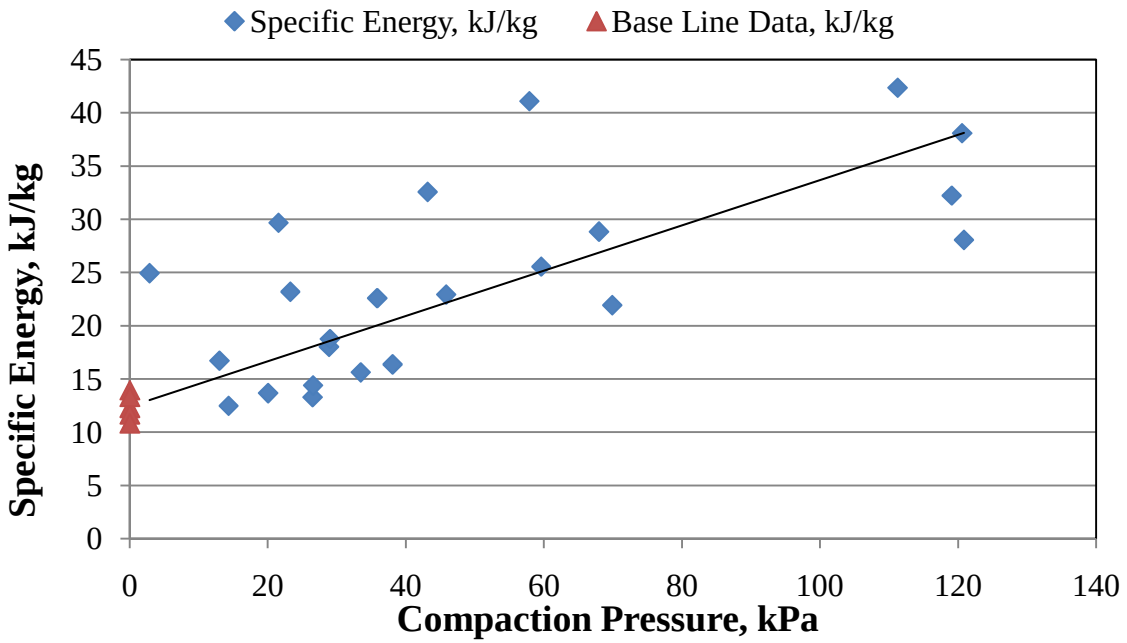

Figure 18. Plot of measured compaction pressure vs. specific energy and regression line based on theoretical specific energy model (shown as solid line).

To account for the torque from friction the torque was plotted against the displacement of the ram. If friction was a major factor in the energy there should have been a noticeable increase in torque as the ram displacement grew. As no noticeable increase was observed it was concluded that the friction component of the specific energy was negligible and left out of the subsequent regression.

The plot of specific energy vs. compaction pressure shows a grouping of points above the model, around the model and below the model. The groups tend to be based on repetitions of the tests, with the specific energy requirement being lower for the later repetitions. The trend can be explained by changes in the material properties over time, or by the machine wearing in.

The baseline energies were collected by simply conveying a measured amount of corn stover through the auger unit of the compacter without the collection tube attached. This provided true 0 kPa data and a basis for evaluating the conveying energy. A non-linear regression of the data yielded a statistically significant relationship. The results of the regression are shown in table 7 below.

Table 7. Parameter estimates for the specific energy vs pressure model.

Model	Regression	Model Parameters	R^2
Specific Energy	Non-Linear	2	0.625
Parameter	Value	Standard Error	P-value
$\tau_C \cos\phi$	1.504 kPa	0.1571	<.0001
μ_F	0.851	$8.90*10^{-3}$	<.0001

The specific energy from conveying was assessed during the baseline tests. Without the compaction tube, the only energy used was in conveying the material the length of the auger unit. The specific energy was found to be 12.419 kJ/kg for conveying. The Degirmencioglu model for specific energy yielded 0.289 kJ/kg for the given dimensions of the system. The Degirmencioglu model was constructed based on conveying grain, which behaves differently in an auger than fibrous materials such as corn stover.

Zhong and O'Callaghan's tests were conducted using fibrous material and a shorter auger with a smaller diameter. By adjusting Zhong and O'Callaghan's findings to match the same length of the auger unit, a specific energy of 181.6 kJ/kg is found. The difference in values can be attributed to the smaller auger diameter in relationship to the particle size of the material being conveyed. The larger particles do not have enough space in a small auger to move around and flow through efficiently.

An auger compacter can be viewed as a baler only with the compaction force coming from an auger rather than a plunger. Comparing the specific energies of baling, 2.88 to 5.76 kJ/kg, to auger compaction shows the latter to be a more energy intensive process. However the specific energies for baling do not include the energy used in chopping and raking the material to prepare it for baling.

A variable pitch auger was constructed using individual flighting sections. The following pitch progression was used: 304.8mm – 254mm – 203.2mm – 152.4mm – 101.6mm. This particular progression was effective at compacting the material between the flights. However the torque requirements were very high and a successful test was never completed. While unplugging the auger after a stalled test the material was found to be packed extremely tight between the flights.

Conclusions and Recommendations

Densification of corn stover using an auger compactor is a competitive technology. Results show that a significant increase in density can be achieved without expending extra energy.

Compacted densities of between 186.9 kg/m^3 and 342.6 kg/m^3 were achieved. The density needed to optimize shipping costs, 234.6 kg/m^3, falls within this range. Relaxed densities up to 235.2 kg/m^3 were achieved with a compaction pressure of 116.85 kPa, resulting in transportation optimization without binding. No formal tests have been conducted concerning the durability of the stover after densification without any binding. However, observations during testing showed a very low durability, resulting in density reduction from handling.

The specific energies needed to compact stover using and auger compactor vary between 18.3 and 35.2 kJ/kg. These energies are 3.4 times greater than those of large square baling for comparable densities. However, there is extra energy using in baling during the chopping and raking steps of the process. These specific energies are much lower than the 181 to 415 kJ/kg needed to either pelletize or briquette corn stover. An auger compacter's ability to achieve optimizing densities for significantly less energy than other processes makes it a competitive technology in biomass densification.

There is a lot of room for this project to expand and become a viable solution for densification in the budding biomass industry. Recommendations for possible improvements include the following:

- Assess the effects of moisture on the system. Moisture may help the material flow through the machine while also allowing the material to adhere more effectively resulting in a more resilient final product.
- A chute could be added to provide a continuous flow system that has the ability of varying density by controlling the amount of pressure that the chute applies to the material.
- Feeding issues could be addressed by redesigning the hopper geometry and possibly adding a beater to facilitate uniform feeding.
- Providing a shearing surface on the leading edge of the hopper to reduce torque spikes from feeding inconsistencies.
- The durability of the final product should be examined to determine the need for a binder whether it be internal or external.
- Conduct further research on corn stover flow through a variable pitch auger. Possible improvements include adding more torque and trying a less aggressive pitch reduction.

References

Atchison J. E., and J. R. Hettenhaus. 2003. Innovative methods for corn stover collecting, handling, storing and transporting. Golden, CO: NREL

Burmistrova, M. F. 1963. Physicomechanical properties of agricultural crops. Translation IPST/NSF. p. 249.

Degirmencioglu, A., and A. K. Srivastava. 1996. Development of screw conveyor performance models using dimensional analysis. *Trans. ASABE* 39(5): 1757−1763

Dilts, M. D. 2007. Application of the rollermill and hammermill for biomass fractionation. MS thesis. Ames, Iowa: Iowa State University, Department of Agricultural Engineering.

Eriksson, S., and M. Prior. 1990. *The Briquetting of Agricultural Waste for Fuel*. Rome: FAO.

Frohberg, D. D. 2005. Harvest and densification of corn stover biomass. MS thesis. Ames, Iowa: Iowa State University, Department of Agricultural Engineering.

Kaliyan, N., and R. V. Morey. 2007. Roll Press Briquetting of Corn Stover and Switchgrass: A Pilot Scale Continuous Briquetting Study. ASABE Paper No. 076044. St. Joseph, Mich.: ASABE.

Kaliyan, N., and R. V. Morey. 2008. Binding Mechanisms of corn stover and switchgrass in briquettes and pellets. ASABE Paper No. 084282. St. Joseph, Mich.: ASABE.

Kaminski, T. 1989. *Investigation of the Feasibility of Collection, Densification, Storage, Transportation, and Marketing of Agricultural Biomass*. Saskatoon, Saskatchewan: Saskatchewan Research Council.

Mani, S., L. G. Tabil, Jr., and S. Sokhansanj. 2003. Mechanical properties of corn stover grind. *Trans. ASABE* 47(6): 1983−1990

Mani, S., L. G. Tabil, Jr., and S. Sokhansanj. 2004. Grinding performance and physical properties of wheat and barley straws, corn stover and switchgrass. Biomass and Bioenergy 27: 339-352

Merritt, A. S., and R. J. Mair. 2008. Mechanics of tunneling machine screw conveyors: a theoretical model. Ge´otechnique 58(2): 79–94

Rumpf, H. 1962. The strength of granules and agglomerates. In *Agglomeration*, W.A. Knepper, ed., 379-418. New York, NY: John Wiley and Sons.

Sokhansanj, S., and A. F. Turhollow. 2004. Biomass Densification – Cubing Operations and Costs for Corn Stover. *Applied Engineering in Agriculture* 20(4): 495−499

Tuetken, T. J. 2002. Development of corn stover harvesting and densification systems. MS thesis. Ames, Iowa: Iowa State University, Department of Agricultural and Biosystems Engineering.

Turhollow, A.F., and S. Sokhansanj. 2007. Costs of harvesting, storing in a large pile, and transporting corn stover in a wet form. *Trans. ASABE* 23(4): 439-448

USDA. 2008. Crop Production 2007 Summary. USDA-NASS Agricultural Statistics 2008. Washington, D.C.: USDA National Agricultural Statistics Service. Available at: http://usda.mannlib.cornell.edu/usda/current/CropProdSu/CropProdSu-01-11-2008.pdf Accessed on 1/7/2009.

Zhong, Z., and J. R. O'Callaghan. 1990 The effect of the shape of the feed opening on the performance of a horizontal screw conveyor. Journal of Agricultural Engineering Research 46(2): 125-128

Zhou, B., K.E. Ileleji, and G. Ejeta. 2008. Physical Property Relationships of Bulk Corn Stover Particles. ASABE Paper No. 066148.

Acknowledgements

The author wishes to express his appreciation to the individuals who have made this research project possible.

Dr. Stuart Birrell is acknowledged for his service as the author's major professor. His guidance and help throughout the course of the project were invaluable.

Dr. Brian Steward and Dr. Steven Hoff are recognized for their service on the author's POS committee and thanked for their endless suggestions and willingness to help.

Wade Sohm is acknowledged for his assistance in fabrication.

Jeremiah Johnson is thanked for helping to harvest material and also for his insight and ideas.

Lucas Beverlin is thanked for his expertise and willingness to help with the statistical analysis of the data.

The author's family is thanked for all their support over the years; none of this would have been possible without them.

Kathryn Vaagen is thanked for her assistance in testing, accurate record keeping, and for always listening and helping to make things more manageable.